Research Article

Yu-Song Wang, Bai-Kun Chen, Xin Huang, Wei-Jie Ding, Qing-Yang Yue, and Chun-Xiao Liu*

Optical properties and thermal stability of the H^+-implanted Dy^{3+}/Tm^{3+}-codoped GeS_2–Ga_2S_3–PbI_2 chalcohalide glass waveguide

https://doi.org/10.1515/phys-2022-0045
received March 19, 2022; accepted May 06, 2022

Abstract: Optical waveguides play a vital role in the manufacture of various optical devices due to their unique performances and high-degree integration. We report on the preparation and characterization of the planar waveguides in the Dy^{3+}/Tm^{3+}-codoped GeS_2–Ga_2S_3–PbI_2 chalcohalide glass. The waveguide was formed by the 400 keV H^+-ion implantation with a dose of 8×10^{16} ions/cm^2. Its thermal stability was studied by annealing at 260°C for 1 h. The changes in the nuclear energy loss with the implantation depth were simulated by the stopping and range of ions in matter (SRIM 2013). The dark-mode characteristics of the waveguide were measured by the prism coupling method. The refractive index distribution of the optical waveguide was reconstructed by the reflectivity calculation method. The modal profile of the waveguide structure was calculated by the finite-difference beam propagation method (FD-BPM). The thermally stable proton-implanted Dy^{3+}/Tm^{3+}-codoped GeS_2–Ga_2S_3–PbI_2 chalcohalide glass waveguide is expected to be applied in mid-infrared integrated optical devices.

Keywords: Dy^{3+}/Tm^{3+}-codoped GeS_2–Ga_2S_3–PbI_2 chalcohalide glass, optical waveguide, ion implantation, thermal stability

*** Corresponding author: Chun-Xiao Liu,** College of Electronic and Optical Engineering, Nanjing University of Posts and Telecommunications, Nanjing 210023, China; Jiangsu Province Engineering Research Center for Fabrication and Application of Special Optical Fiber Materials and Devices, Nanjing 210023, China, e-mail: chunxiaoliu@njupt.edu.cn
Yu-Song Wang, Bai-Kun Chen, Xin Huang, Wei-Jie Ding: College of Electronic and Optical Engineering, Nanjing University of Posts and Telecommunications, Nanjing 210023, China
Qing-Yang Yue: Shandong Provincial Engineering and Technical Center of Light Manipulations & Shandong Provincial Key Laboratory of Optics and Photonic Device, School of Physics and Electronics, Shandong Normal University, Jinan 250014, China

1 Introduction

As the silicon-based semiconductor process of integrated circuits approaches the theoretical limit, the development of integrated optical circuits provides new possibilities for future information technology. Compared with discrete optical devices, integrated optical elements have the advantages of compact structure, good stability, strong anti-interference and high precision by integrating multi-functional devices [1,2]. As the basis of integrated optical devices, an optical waveguide plays an important role in optical communication and information processing [3]. The waveguide layer with high refractive index can be used to propagate and process optical signals [4]. An optical waveguide is a device that confines the propagation of light waves on its surface or inside [5]. The light propagated in the optical waveguide is generally limited to a small region with micron size, so that it can be propagated in a non-diffractive manner in the cavity [6]. Furthermore, the light intensity in the waveguide layer is far greater than that of the substrate itself, so it has good research value and wide application [7]. The formation of optical waveguides belongs to the category of micro-nano machining. A large number of breakthroughs depend on the improvement in scale and accuracy of micro/nano manufacturing technique. Ion implantation is a booming and widely used material surface modification technology [8–11]. It has the advantages of strong adaptability and good controllability [12–15]. It is used to prepare one-dimensional waveguide structures in this experiment.

The selection of matrix materials for integrated optical components (especially optical waveguides) have attracted widespread scholar's attentions [16–19]. Dy^{3+}/Tm^{3+}-codoped GeS_2–Ga_2S_3–PbI_2 chalcohalide glasses are under consideration for high-quality optical waveguides that can meet the functional requirements of the optoelectronic devices, because of the characteristics of low phonon energy, wide infrared transmittance range, high refractive index, large emission cross-section, high nonlinear refractive

index, long fluorescence lifetime and low melting temperature [20]. Furthermore, the chalcohalide glass itself and the economic cost of its processing are relatively low, which mainly determines the expenditure and practicality of the waveguide as an integrated optical component [21]. The exploration of the Dy^{3+}/Tm^{3+}-codoped GeS_2–Ga_2S_3–PbI_2 chalcohalide glass waveguides by the H^+ ion implantation has not been reported to the best of our knowledge. Furthermore, the thermal stability is a fundamental requirement in the practical application of devices. Therefore, it is necessary to compare the optical properties of the waveguide before and after annealing. In this work, the advanced proton implantation method and the excellent performances of the Dy^{3+}/Tm^{3+}-codoped GeS_2–Ga_2S_3–PbI_2 chalcohalide glass are well combined to prepare high-quality optical waveguides. We test its optical performances and thermal stability through some simulation software and experimental methods. It has simple preparation process and optimum waveguide performances, which can provide theoretical and experimental basis for the preparation of chalcohalide devices and the diversity of optical waveguide structures in integrated optical system.

2 Experiments and simulations

The Dy^{3+}/Tm^{3+}-codoped GeS_2–Ga_2S_3–PbI_2 chalcohalide glass was prepared in the Xi'an Institute of Optics and Precision Mechanics of Chinese Academy of Sciences (CAS). The size of the sample is 10.0 mm × 5.0 mm × 1.0 mm. The samples were optically polished before any experiment.

For preparing the planar waveguide structure, the surface of the Dy^{3+}/Tm^{3+}-codoped GeS_2–Ga_2S_3–PbI_2 chalcohalide glass was bombarded by a 400 keV H^+ ion beam with a dose of 8×10^{16} ions/cm^2 at room temperature. The ion implantation process is shown in Figure 1. In order to avoid the channel effect, the normal direction of the Dy^{3+}/Tm^{3+}-codoped GeS_2–Ga_2S_3–PbI_2 chalcohalide glass surface maintained an angle of 7° from the direction of the incident ion beam. The ion current density was limited to 50 nA/cm^2 to prevent thermal effect. Then, a planar optical waveguide structure was formed on the Dy^{3+}/Tm^{3+}-codoped GeS_2–Ga_2S_3–PbI_2 chalcohalide glass.

After the ion implantation, the waveguide sample was annealed at 260°C for 1 h to study the thermal stability of the waveguide, taking into account its transition temperature. The prism coupling system was used to record the m-line curve with the effective refractive index of the mode before and after the annealing. The refractive index profile can affect the guiding properties of the optical waveguide. However, it is difficult to directly measure the refractive index profile. Chandel and Lama in 1986 proposed a method for calculating the refractive index profile of waveguides, which is called Reflectivity Calculation Method (RCM). In order to obtain a reasonable refractive index profile, it is necessary to constantly adjust the parameters of the assumed function that consists of the two semi-Gaussian curves with different standard deviations during the RCM simulation process to reduce excessive differences between the calculated effective refractive index and the measured one. By continuously adjusting the parameter values, the differences between the simulation results of the assumed refractive index profile and the experimental results are controlled within the allowable range (for example, on the order of 10^{-3}). The function curve at this time represents the actual refractive index distribution of the waveguide.

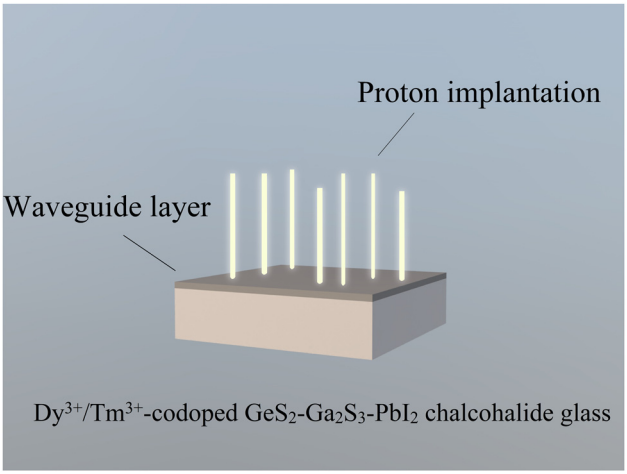

Figure 1: Schematic diagram of the ion implantation process.

3 Results and discussions

The Stopping and Range of Ions in Matter (SRIM 2013) was utilized to stimulate the depth distribution of the energy loss for the 400 keV hydrogen ion implantation into the Dy^{3+}/Tm^{3+}-codoped GeS_2–Ga_2S_3–PbI_2 chalcohalide glass [22]. Figure 2 shows the nuclear energy loss as a function of the implantation depth [23]. First, it increases slowly in the main implantation range of 0–3 μm. Then, the nuclear energy loss reaches rapidly to the maximum value of 1.26 keV/μm at the depth of 3.99 μm. Finally, it quickly drops to zero. When the implanted ions enter into the deeper area from the sample surface, they stop

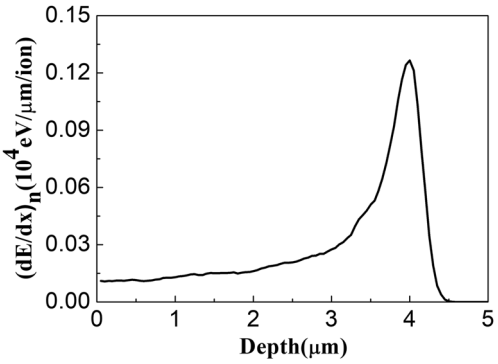

Figure 2: Nuclear energy loss of the 400 keV proton implantation into the Dy^{3+}/Tm^{3+}-codoped GeS_2–Ga_2S_3–PbI_2 chalcohalide glass.

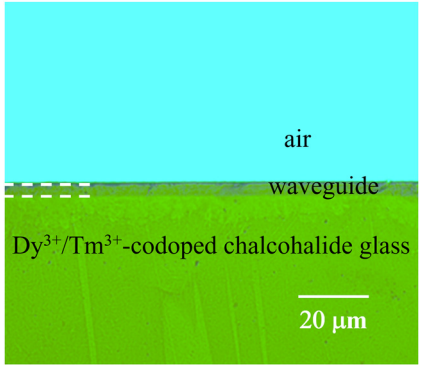

Figure 3: Microscope image of the cross-section of the proton-implanted Dy^{3+}/Tm^{3+}-codoped GeS_2–Ga_2S_3–PbI_2 chalcohalide glass.

moving owing to the energy loss caused by the elastic collision with the atomic nucleus of the target material. The density of the area where the ions are accumulated is decreased, and hence an optical barrier [19,20] structure is formed here. The results indicate that the deposition of nuclear energy promotes the formation of the optical barrier and changes the distribution of the refractive index.

Figure 3 shows the cross-sectional microscopic image of the proton-implanted Dy^{3+}/Tm^{3+}-codoped GeS_2–Ga_2S_3–PbI_2 chalcohalide glass, which was observed by a metallographic microscope (Axio Imager A2m) with a magnification of ×500. The region between the air and the substrate is the waveguide layer. Light can be effectively limited in the vertical direction and propagated in this region. The thickness of the waveguide layer is about 4.0 μm, which is almost the same as the theoretical simulation of SRIM 2013 software in Figure 2. The substrate and the waveguide layer have some defects, which are caused by the rough polishing.

The dark-mode curve (relative intensity of light versus effective refractive index) was measured by the prism-coupling system that possesses a Gaussian single-mode light beam from He–Ne laser at 632.8 nm with a diameter of 0.2 mm at TE polarization. Figure 4(a) and (b) shows the characteristics of the dark modes in the proton-implanted Dy^{3+}/Tm^{3+}-codoped GeS_2–Ga_2S_3–PbI_2 chalcohalide glass waveguide before and after the annealing treatment at 260°C for 1 h, respectively. There are two sharp dips and one broad dip on the m-line curves of both the as-implanted and annealed chalcohalide glass waveguides. The first dip is sharp and narrow, which represents a propagation mode (the fundamental mode) [24,25]. When the incident laser beam is totally reflected at the bottom of the prism and the incident light meets the phase matching condition (the wave vector of light propagating in the *z*-direction in the prism is equal to that in the waveguide layer), the light will enter into the waveguide layer through the air gap. Hence, lack of reflected light results in a sharp drop in the light intensity. The second dip is relatively narrow and is the other guided mode. The third dip is really smooth and indicates a leaky mode formed by the multiple optical reflections. As shown in Figure 4, with the increase in the mode number, the width of dips in the dark-mode spectrum becomes broader. It indicates that

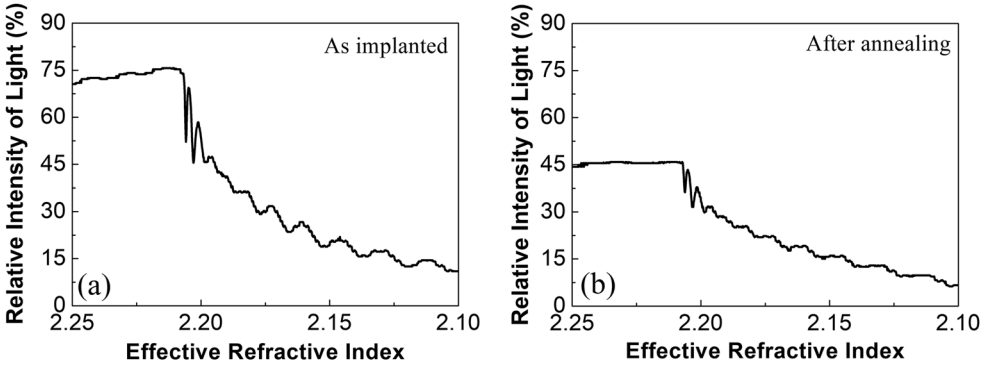

Figure 4: The m-line spectra of the (a) as-implanted and (b) annealed Dy^{3+}/Tm^{3+}-codoped GeS_2–Ga_2S_3–PbI_2 chalcohalide glass waveguide.

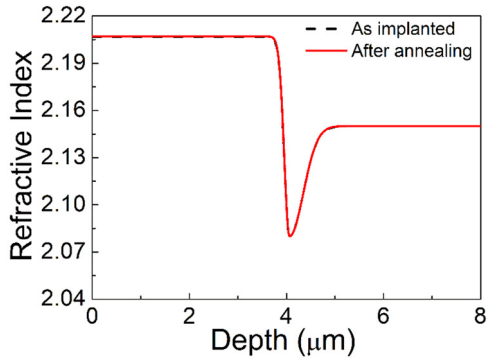

Figure 5: Refractive index distributions of the optical waveguide before and after annealing.

Table 1: Measured and calculated effective refractive indices of the modes in the H^+-implanted Dy^{3+}/Tm^{3+}-codoped GeS_2–Ga_2S_3–PbI_2 chalcohalide glass waveguide before and after annealing

Mode	Effective refractive index					
	As-implanted			After annealing		
	Exp.	Cal.	Diff.	Exp.	Cal.	Diff.
TE_0	2.2057	2.2055	2.0×10^{-4}	2.2063	2.2057	6.0×10^{-4}
TE_1	2.2029	2.2014	1.5×10^{-3}	2.2030	2.2016	1.4×10^{-3}
TE_2	2.1982	2.1945	3.7×10^{-3}	2.1988	2.1947	4.1×10^{-3}

the ability of the optical waveguide to limit the propagation of higher order modes is weakening and the higher order modes may become leaky modes. By comparing the effective refractive index of the mode with the substrate, we can find that the effective refractive index in the near-surface region is larger than that of the substrate (n_{sub} = 2.15) after the implantation of protons into the Dy^{3+}/Tm^{3+}-codoped GeS_2–Ga_2S_3–PbI_2 chalcohalide glass. It indicates that the "well-enhanced" waveguide structure with high refractive index is formed by the ion implantation. Comparing Figure 4(a) with (b), neither the shape of the dark-mode curve nor the effective refractive index of each dark mode is affected by the annealing process for the Dy^{3+}/Tm^{3+}-codoped GeS_2–Ga_2S_3–PbI_2 chalcohalide glass waveguide. Therefore, the dark-mode properties can be well preserved after the thermal treatment.

Based on the effective refractive indices obtained from the dark-mode curve, we utilized the RCM [26] software to reconstruct the refractive index distributions of the proton-implanted Dy^{3+}/Tm^{3+}-codoped GeS_2–Ga_2S_3–PbI_2 chalcohalide glass waveguide at 632.8 nm before and after the annealing treatment, as shown in Figure 5. There is a slight increase (Δn_w = +0.0569) in refractive index in the waveguide layer and a small drop (Δn_b = −0.07) in refractive index at the optical barrier layer. Therefore, the waveguide is a typical "well enhanced + optical barrier" type. The depth of the optical barrier calculated by the RCM is 4.07 μm, which is close to the datum of 3.99 μm calculated by the SRIM 2013 simulation. Table 1 lists the differences between the experimental and calculated effective refractive indices for the hydrogen-ion implanted Dy^{3+}/Tm^{3+}-codoped GeS_2–Ga_2S_3–PbI_2 chalcohalide glass waveguide. It can be seen that the difference between two values is controlled between 10^{-4} and 10^{-3}, which proves that the RCM simulation result is reasonable. The reconstructed refractive index profile at 632.8 nm can be used to

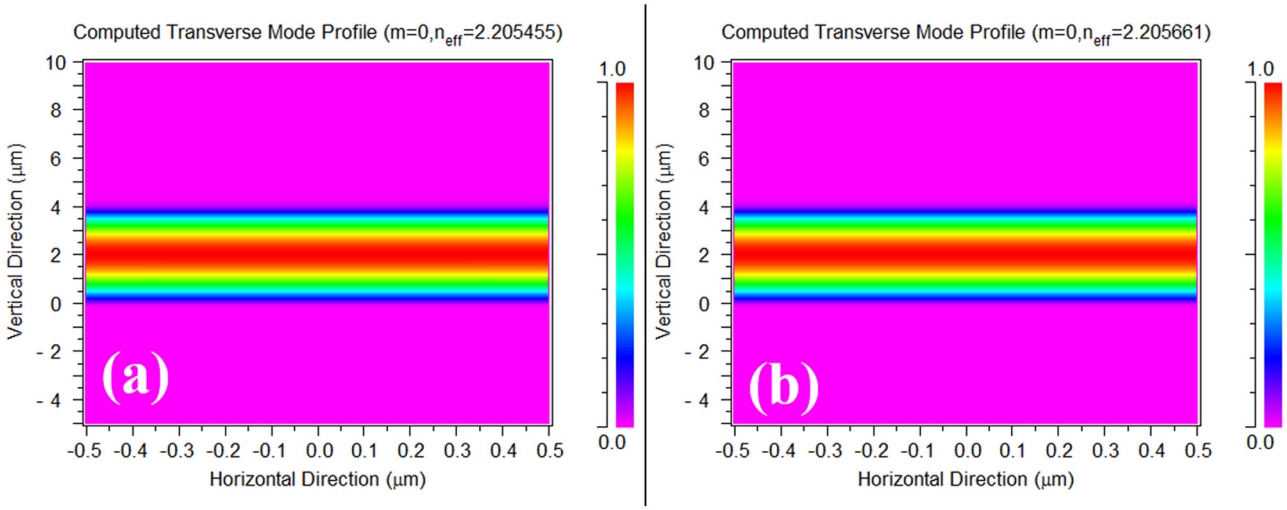

Figure 6: Near-field light intensity distributions simulated by the FD-BPM (a) before and (b) after annealing.

investigate the optical properties of the waveguide. In addition, the annealing treatment hardly changed the increment in the refractive index in the waveguide region and the reduction in the refractive index in the barrier layer. Therefore, the refractive index distribution is stable at the temperature of 260°C.

In order to detect the propagation quality of the optical waveguide, we adopted the finite-difference beam propagation method (FD-BPM) to simulate the near-field light intensity distribution at 632.8 nm [27,28]. Figure 6(a) and (b) show the FD-BPM-calculated near-field light intensity distributions for the as-implanted and annealed proton-implanted Dy^{3+}/Tm^{3+}-codoped GeS_2–Ga_2S_3–PbI_2 chalcohalide glass waveguide, respectively. The n_{eff} of the fundamental mode in the computed transverse mode profiles are 2.205455 and 2.205661 before and after the thermal treatment, which are almost the same as their counterparts listed in Table 1. The width of the simulated near-field intensity profile is about 4.0 μm, which is consistent with the implantation depth. It manifested the excellent competence of confining the propagation of light perpendicular to the waveguide layer without light leakage. Comparing Figure 6(a) with Figure 6(b), the parameters including the light intensity distribution and the effective refractive index of the fundamental mode in the as-implanted waveguide are similar to those in the annealed one. It suggests that the near-field light intensity distribution can remain stable at the temperature of 260°C in air.

4 Conclusion

One-dimensional waveguide structure was fabricated by the 400 keV H^+-ion implantation with a dose of 8×10^{16} ions/cm^2 in the Dy^{3+}/Tm^{3+}-codoped GeS_2–Ga_2S_3–PbI_2 chalcohalide glass. The dark-mode spectrum demonstrates that there are three guided modes. The refractive index distribution of the waveguide simulated by the RCM suggests that the refractive index distribution is an "well enhanced + optical barrier" type with the maximum refractive index difference of 0.1269. The near-field light intensity distribution calculated by the FD-BPM manifests that the waveguide can well limit the light propagation. The optical waveguide has thermal stability within the temperature of 260°C by discussing the changes in their dark-mode curves, refractive index distributions and the modal profiles. It provides a reference for the further development of the mid-infrared chalcohalide glass photonics devices.

Funding information: The authors acknowledge the support from the National Natural Science Foundation of China (Grant No. 11405041), and the Scientific Research Foundation for Youths Supported by Jiangxi Province Science Foundation (Grant No. 20192BAB217015).

Author contributions: All authors have accepted responsibility for the entire content of this manuscript and approved its submission.

Conflict of interest: The authors state no conflict of interest.

References

[1] Ríos C, Stegmaier M, Hosseini P, Wang D, Scherer T, Wright CD, et al. Integrated all-photonic non-volatile multi-level memory. Nat Pho. 2015;9(11):725. doi: 10.1038/NPHOTON.2015.182.
[2] Wang C, Zhang M, Chen X, Bertrand M, Shams-Ansari A, Chandrasekhar S, et al. Integrated lithium niobate electro-optic modulators operating at CMOS-compatible voltages. Nature. 2018;562(7725):101. doi: 10.1038/s41586-018-0551-y.
[3] Wang CX, Yao YC, Tan Y. Ion irradiated magneto-optic waveguide based on TGG crystal. Opt Mater Exp. 2019;9(3):1128–35. doi: 10.1364/OME.9.001128.
[4] Tervonen A, West BR, Honkanen S. Ion-exchanged glass waveguide technology: a review. Opt Eng. 2011;50(7):071107. doi: 10.1117/1.3559213.
[5] He S, Yang QX, Zhang B, Ren YY, Liu HL, Wu PF, et al. A waveguide mode modulator based on femtosecond laser direct writing in KTN crystals. Results Phys. 2020;18:103307. doi: 10.1016/j.rinp.2020.103307.
[6] Jia CL, Li S, Song XX. Optical and structural properties of Nd: MgO: $LiNbO_3$ crystal irradiated by 2.8-MeV He ions. Appl Phys B. 2017;123(7):206. doi: 10.1007/s00340-017-6783-y.
[7] Kip D. Photorefractive waveguides in oxide crystals: fabrication, properties, and applications. Appl Phys B. 1998;67(2):131–50. doi: 10.1007/s003400050485.
[8] Zhang J, Chen JY, Zhang LL, Lin SB, Liu CX. Bismuth-doped phosphate glasses and H^+-implanted waveguides. J Korean Phys Soc. 2020;76(6):479–83. doi: 10.3938/jkps.76.479.
[9] Bai MY, Zhao YL, Jiao BB, Zhu LJ, Zhang GD, Wang L. Research on ion implantation in MEMS device fabrication by theory, simulation and experiments. Int J Mod Phys B. 2018;32(14):1850170. doi: 10.1142/S0217979218501709.
[10] Wang LL, Cui XJ, Liu NQ. Effect of He^+ ion implantation on Rb^+-K^+ exchanged $KTiOPO_4$ optical waveguide. Mod Phys Lett B. 2018;32(24):1850288. doi: 10.1142/S0217984918502883.
[11] Zhao JH, Ye LL, Jiao XS, Yue QY, Liu Y. The damage investigations of 4H-SiC after P ion irradiation. Appl Phys A. 2020;126(7):531. doi: 10.1007/s00339-020-03722-z.
[12] Liu P, Huang Q, Liu T, Guo SS, Zhang L, Wang XL. Nd: $Li_6Y(BO_3)_3$ crystal waveguide properties at wavelengths of 633 and 1,539 nm produced by oxygen or silicon ion implantation. Appl Opt. 2012;51(11):1681–7. doi: 10.1364/AO.51.001681.
[13] Chen F. Micro- and submicrometric waveguiding structures in optical crystals produced by ion beams for photonic

applications. Laser Photon Rev. 2012;6(5):622–40. doi: 10.1002/lpor.201100037.
[14] Bányász I, Zolnai Z, Fried M, Berneschi S, Pelli S, Nunzi-Conti G. Leaky mode suppression in planar optical waveguides written in Er:TeO_2-WO_3 glass and CaF_2 crystal via double energy implantation with MeV N^+ ions. Nucl Instrum Methods Phys Res B. 2014;326:81–5. doi: 10.1016/j.nimb.2013.10.039.
[15] Vázquez GV, Valiente R, Gómez-Salces S, Flores-Romero E, Rickards J, Trejo-Luna R. Carbon implanted waveguides in soda lime glass doped with Yb^{3+} and Er^{3+} for visible light emission. Opt Laser Technol. 2016;79:132–6. doi: 10.1016/j.optlastec.2015.12.002.
[16] Cheng YZ, Lv JM, Akhmadaliev S, Zhou SQ, Chen F. Optical ridge waveguides in Nd: LGS crystal produced by combination of swift C^{5+} ion irradiation and precise diamond blade dicing. Opt Laser Technol. 2016;81:122–6. doi: 10.1016/j.optlastec.2016.02.009.
[17] Liu CX, Zhang J, Lin SB, Yue QY, Zheng RL, Guo JH. Two-dimensional waveguides in magneto-optical glasses fabricated by carbon ion implantation and femtosecond laser ablation. Opt Commun. 2021;495:127109. doi: 10.1016/j.optcom.2021.127109.
[18] Zhang J, Chen JY, Lu Y, Wang YS, Zhang LL, Yue QY, et al. Optical planar and ridge waveguides in terbium scandium aluminum garnet crystal fabricated by ion implantation and precise diamond blade dicing. Vacuum. 2021;193:110493. doi: 10.1016/j.vacuum.2021.110493.
[19] Liu FR, Liu T, Yao YC, Liu Y, Kong WJ, Cheng L, et al. Lattice structures and optical properties of Ce: LYSO crystal waveguides with implanted C, Si and Cu ions. J Lumin. 2022;242:118559. doi: 10.1016/j.jlumin.2021.118559.
[20] Ashok N, Lee YL, Shin WJ. Chalcogenide waveguide structure for dispersion in mid-infrared wavelength. Jpn J Appl Phys. 2017;56(3):032501. doi: 10.7567/JJAP.56.032501.
[21] Chen JY, Zhou Q, Wang Y, Zhu QF, Tang ZL, Guo HT, et al. Characterization of optical waveguide in chalcogenide glass formed by helium ion implantation. Indian J Phys. 2021;95(6):1239–43. doi: 10.1007/s12648-020-01768-6.
[22] Ziegler JF. SRIM-the stopping and range of ions in matter. http://www.srim.org.
[23] Yan ZF, Zhang ZH, Xu SY, Ma JX, Hou YS, Ji YC. Nuclear radiation detection based on the convolutional neural network under public surveillance scenarios. Open Phys. 2022;20(1):49–57. doi: 10.1515/phys-2022-0006.
[24] Zhang J, Chen JY, Zhang LL, Lin SB, Liu CX. Bismuth-doped phosphate glasses and H^+ -implanted waveguides. J Korean Phy Soc. 2020;76(6):479–83. doi: 10.3938/jkps.76.479.
[25] Liu CX, You JL, Lin SQ, Chen JY, Tang M, Lin SB, et al. A ridge waveguide constructed by H^+ implantation and precise diamond blade dicing in high-gain Nd^{3+} -doped laser glass. Optik. 2021;225:165881. doi: 10.1016/j.ijleo.2020.165881.
[26] Chandler JP, Lama FL. A new approach to the determination of planar waveguide profiles by means of a nonstationary mode index calculation. Opt Acta. 1986;33(2):127–43. doi: 10.1080/713821921.
[27] Rsoft Design Group. Computer software BeamPROP version 8.0. http://www.rsoftdesign.com.
[28] Lv JY, Guo HT, Xu J, Liu CX. Near-infrared properties of optical planar waveguides formed by H^+ ion implantation in Yb^{3+}-doped phosphate glasses. Acta Photon Sin. 2020;49(4):0423001. doi: 10.3788/gzxb20204904.0423001.